

2.7: Electrochemistry

Cyclic Voltammetry Measurements

Introduction

Cyclic voltammetry (CV) is one type of potentiodynamic electrochemical measurements. Generally speaking, the operating process is a potential-controlled reversible experiment, which scans the electric potential before turning to reverse direction after reaching the final potential and then scans back to the initial potential, as shown in Figure 2.7.1 -a . When voltage is applied to the system changes with time, the current will change with time accordingly as shown in Figure 2.7.1 -b. Thus the curve of current and voltage, illustrated in Figure 2.7.1 -c, can be represented from the data, which can be obtained from Figure 2.7.1 -a and Figure 2.7.1 -b.

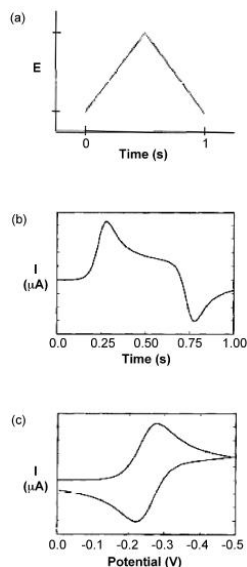


Figure 2.7.1 Potential wave changes with time (a); current response with time (b); current-potential representations (c). Adapted from D. K. Gosser, Jr. *Cyclic Voltammetry Simulation and Analysis of Reaction Mechanisms*, Wiley-VCH, New York, (1993).

Cyclic voltammetry is a very important analytical characterization in the field of electrochemistry. Any process that includes electron transfer can be investigated with this characterization. For example, the investigation of catalytical reactions, analyzing the stoichiometry of complex compounds, and determining of the photovoltaic materials' band gap. In this module, I will focus on the application of CV measurement in the field of characterization of solar cell materials.

Although CV was first practiced using a hanging mercury drop electrode, based on the work of Nobel Prize winner Heyrovský (Figure 2.7.2), it did not gain widespread until solid electrodes like Pt, Au and carbonaceous electrodes were used, particularly to study anodic oxidations. A major advance was made when mechanistic diagnostics and accompanying quantitations became known through the computer simulations. Now, the application of computers and related software packages make the analysis of data much quicker and easier.



Figure 2.7.2 Czech chemist and inventor Jaroslav Heyrovský (1890 – 1967).

The Components of a CV System

As shown in Figure 2.7.3, the CV systems are as follows:

- The epsilon includes potentiostat and current-voltage converter. The potentiostat is required for controlling the applied potential, and a current-to-voltage converter is used for measuring the current, both of which are contained within the epsilon (Figure 2.7.3).
- The input system is a function generator (Figure 2.7.3). Operators can change parameters, including scan rate and scan range, through this part. The output part is a computer screen, which can show data and curves directly to the operators.
- All electrodes must work in electrolyte solution.
- Sometimes, the oxygen and water in the atmosphere will dissolve in the solution, and will be deoxidized or oxidized when voltage is applied. Therefore the data will be less accurate. To prevent this from happening, bubbling of an inert gas (nitrogen or argon) is required.
- The key component of the CV systems is the electrochemical cell which is connected to the epsilon part. Electrochemical cell contains three electrodes, counter electrode (C in Figure 2.7.3) working electrode (W in Figure 2.7.3) and reference electrode (R in Figure 2.7.3). All of them must be immersed in an electrolyte solution when working.

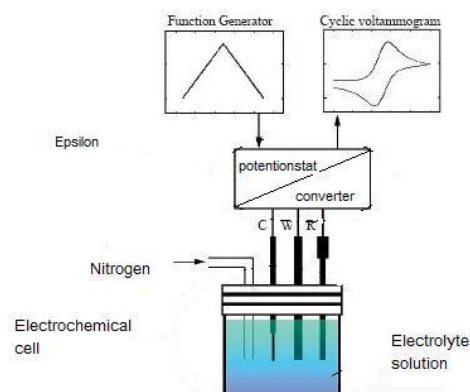


Figure 2.7.3 Components of cyclic voltammetry systems. Adapted from D. K. Gosser, Jr., *Cyclic Voltammetry Simulation and Analysis of Reaction Mechanisms*, Wiley-VCH, New York, (1993).

In order to better understand the electrodes mentioned above, three kinds of electrodes will be discussed in more detail.

- Counter electrodes (C in Figure 2.7.3) are non-reactive high surface area electrodes, for which the platinum gauze is the common choice.
- The working electrode in (W in Figure 2.7.3) is commonly an inlaid disc electrodes (Pt, Au, graphite, etc.) of well-defined area are most commonly used. Other geometries may be available in appropriate circumstances, such as dropping or hanging mercury hemisphere, cylinder, band, arrays, and grid electrodes.
- For the reference electrode (R in Figure 2.7.3) aqueous Ag/AgCl or calomel half cells are commonly used, and can be obtained commercially or easily prepared in the laboratory. Sometimes, a simple silver or platinum wire is used in conjunction with an

internal potential reference provided by ferrocene, when a suitable conventional reference electrode is not available. Ferrocene undergoes a one-electron oxidation at a low potential, around 0.5 V versus a saturated calomel electrode (SCE). It is also been used as standard in electrochemistry as $F_c^+/F_c = 0.64$ V versus a normal hydrogen electrode (NHE).

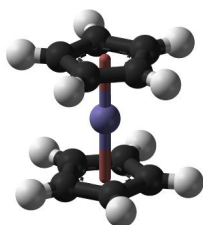


Figure 2.7.4 The structure of $(C_5H_5)_2Fe$ (ferrocene).

Cyclic voltammetry systems employ different types of potential waveforms (Figure 2.7.4) that can be used to satisfy different requirements. Potential waveforms reflect the way potential is applied to this system. These different types are referred to by characteristic names, for example, cyclic voltammetry, and differential pulse voltammetry. The cyclic voltammetry analytical method is the one whose potential waveform is generally an isosceles triangle (Figure 2.7.4 a).

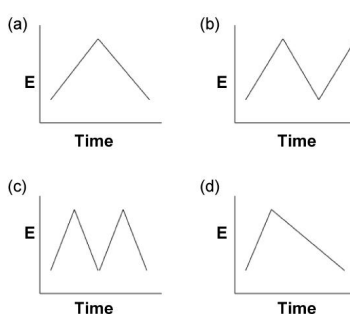


Figure 2.7.5 Examples of different waveforms of CV systems, illustrating various possible cycles. Adapted from D. K. Gosser, Jr., *Cyclic Voltammetry Simulation and Analysis of Reaction Mechanisms*, Wiley-VCH, New York (1993).

Physical Principles of CV Systems

As mentioned above, there are two main parts of a CV system: the electrochemical cell and the epsilon. Figure 2.7.6 shows the schematic drawing of circuit diagram in electrochemical cell.

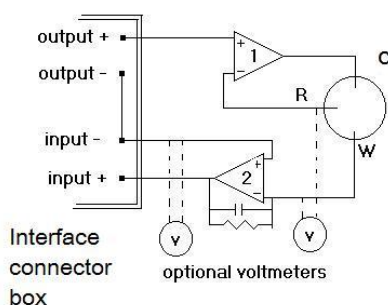


Figure 2.7.6 Diagram of a typical cyclic voltammetry circuit layout. Adapted from R. G. Compton and C. E. Banks, *Understanding Voltammetry*, World Scientific, Singapore (2007).

In a voltammetric experiment, potential is applied to a system, using working electrode (W in Figure 2.7.7) and the reference electrode (R = Figure 2.7.7) and the current response is measured using the working electrode and a third electrode, the counter electrode (C in Figure 2.7.7). The typical current-voltage curve for ferricyanide/ferrocyanide, 2.7.1, is shown in Figure 2.7.7.

$$E_{eq} = E^{\circ} + (0.059/n) \log([reactant]/[product]) \quad (2.7.1)$$

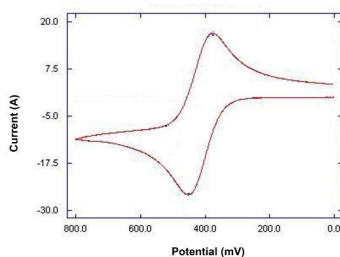


Figure 2.7.7 Typical curve of current-voltage curve for for ferricyanide/ferrocyanide, 2.7.1 .

What Useful Information Can We Get From The Data Collected

The information we are able to obtain from CV experimental data is the current-voltage curve. From the curve we can then determine the redox potential, and gain insights into the kinetics of electron reactions, as well as determine the presence of reaction intermediate.

Why CV For The Characterizations Of Solar Cell Materials

Despite some limitations, cyclic voltammetry is very well suited for a wide range of applications. Moreover, in some areas of research, cyclic voltammetry is one of the standard techniques used for characterization. Due to its characteristic shapes of curves, it has been considered as ‘electrochemical spectroscopy’. In addition, the system is quite easy to operate, and sample preparation is relatively simple.

The band gap of a semiconductor is a very important value to be determined for photovoltaic materials. Figure 2.7.8 shows the relative energy level involved in light harvesting of an organic solar cell. The energy difference (E_g) between the lowest unoccupied molecular orbital (LUMO) and the highest occupied molecular orbital (HOMO), which determines the efficiency. The oxidation and reduction of an organic molecule involve electron transfers (Figure 2.7.9), and CV measurements can be used to determine the potential change during redox. Through the analysis of data obtained by the CV measurement the electronic band gap is obtained.

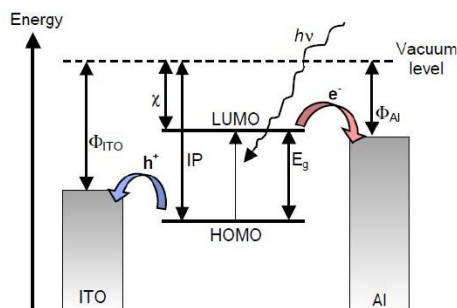


Figure 2.7.8 Diagram showing energy level and light harvesting of an organic solar cell. Adapted from S. B. Darling, *Energy Environm. Sci.*, 2009, 2, 1266.

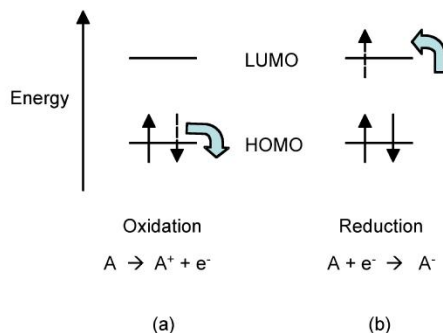


Figure 2.7.9 Diagram showing energy level and light harvesting of organic solar cell. Adapted from D. K. Gosser, Jr., *Cyclic Voltammetry Simulation and Analysis of Reaction Mechanisms*, Wiley-VCH, New York (1993).

The Example Of The Analysis Of CV Data In Solar Cell Material Charecterization

Graphene nanoribbons (GNRs) are long, narrow sheets of graphene formed from the unzipping of carbon nanotubes (Figure 2.7.10). GNRs can be both semiconducting and semi-metallic, depending on their width, and they represent a particularly versatile variety of graphene. The high surface area, high aspect ratio, and interesting electronic properties of GNRs render them promising candidates for applications of energy-storage materials.

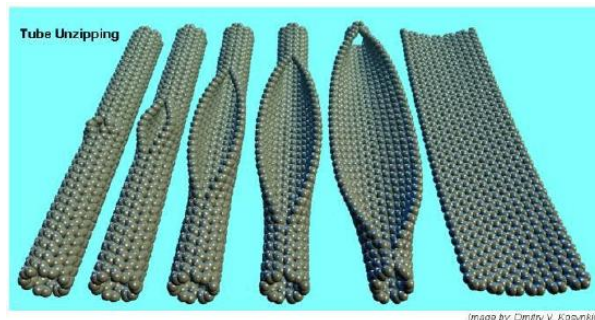


Figure 2.7.10 Schematic for the “unzipping” of carbon nanotubes to produce graphene (Rice University).

Graphene nanoribbons can be oxidized to oxidized graphene nanoribbons (XGNRs), are readily soluble in water easily. Cyclic voltammetry is an effective method to characterize the band gap of semiconductor materials. To test the band gap of oxidized graphene nanoribbons (XGNRs), operating parameters can be set as follows:

- 0.1M KCl solution
- Working electrode: evaporated gold on silicon.
- Scan rate: 10 mV/s.
- Scan range: 0 ~ 3000 mV for oxidization reaction; -3000 ~ 0 mV for reduction reaction.
- Samples preparation: spin coat an aqueous solution of the oxidized graphene nanoribbons onto the working electrode, and dry at 100 °C.

To make sure that the results are accurate, two samples can be tested under the same condition to see whether the redox peaks are at the same position. The amount of XGNRs will vary from sample to sample, thus the height of peaks will vary also. Typical curves obtained from the oxidation reaction (Figure 2.7.9 a) and reduction reaction (Figure 2.7.9 b) are shown in Figure 2.7.10 and Figure 2.7.11, respectively.

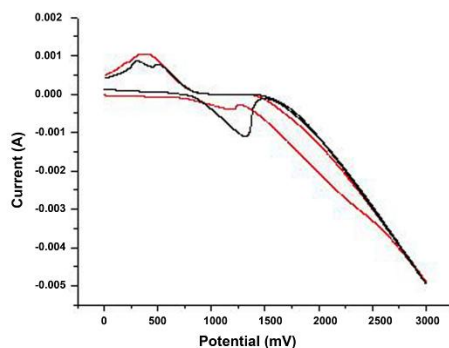


Figure 2.7.11 Oxidation curves of two samples of XGNRs prepared under similar condition. The sample with lower concentration is shown by the red curve, while the sample with higher concentration is shown as a black curve.

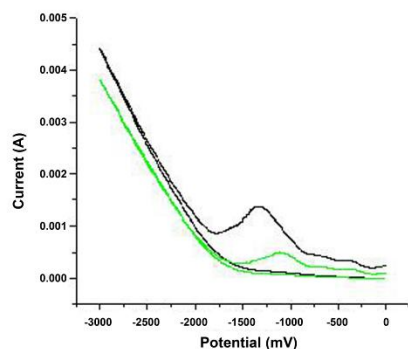


Figure 2.7.12 Reduction curves of two samples of XGNRs prepared under similar condition. The sample with lower concentration is shown by the green curve, while the sample with higher concentration is shown as a black curve.

From the curves shown in Figure 2.7.11 and Figure 2.7.12 the following conclusions can be obtained:

- Two reduction peak and onset is about -0.75 eV (i.e. Figure 2.7.9 b).
- One oxidation peak with onset about 0.85 eV (i.e. Figure 2.7.9 a).
- The calculated band gap = 1.60 eV

In conclusion, there are many applications for CV system, efficient method, and the application in the field of solar cell provides the band gap information for research.

Applications of Cyclic Voltammetry in Proton Exchange Membrane Fuel Cells

Introduction

Proton exchange membrane fuel cells (PEMFCs) are one promising alternative to traditional combustion engines. This method takes advantage of the exothermic hydrogen oxidation reaction in order to generate energy and water (Table 2.7.1).

Table 2.7.1 Summary of oxidation-reduction reactions in PEMFC in acidic and basic electrolytes.

| | Acidic Electrolyte | Acidic Redox Potential at STP (V) | Basic Electrolyte | Basic Redox Potential at STP (V) |
|------------------------------|---------------------------------------|-----------------------------------|---|----------------------------------|
| Anode half-reaction | $2H_2 \rightarrow 4H^+ + 4e^-$ | | $2H_2 + 4OH^- \rightarrow 4H_2O + 4e^-$ | |
| Cathode half-reaction | $O_2 + 4e^- + 4H^+ \rightarrow 2H_2O$ | 1.23 | $O_2 + 4e^- + 2H_2O \rightarrow 4OH^-$ | 0.401 |

The basic PEMFC consists of an anode and a cathode separated by a proton exchange membrane (Figure 2.7.13). This membrane is a key component of the fuel cell because for the redox couple reactions to successfully occur, protons must be able to pass from the anode to the cathode. The membrane in a PEMFC is usually composed of Nafion, which is a polyfluorinated sulfonic acid, and exclusively allows protons to pass through. As a result, electrons and protons travel from the anode to the cathode through an external circuit and through the proton exchange membrane, respectively, to complete the circuit and form water.

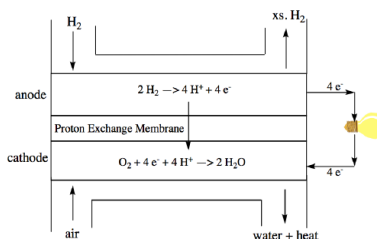


Figure 2.7.13 Schematic of a proton exchange membrane fuel cell (PEMFCs).

PEMFCs present many advantages compared to traditional combustion engines. They are more efficient and have a greater energy density than traditional fossil fuels. Additionally, the fuel cell itself is very simple with few or no moving parts, which makes it long-lasting, reliable, and very quiet. Most importantly, however, the operation of a PEMFC results in zero emissions as the only byproduct is water (Table 2.7.2). However, the use of PEMFCs has been limited because of the slow reaction rate for the oxygen

reduction half-reaction (ORR). Reaction rates, k° , for reduction-oxidation reactions such as these tend to be on the order of 10^{-10} – 10^{-9} where 10^{-10} is the fastest reaction rate and 10^{-9} is the slowest reaction rate. Compared to the hydrogen oxidation half-reaction (HOR), which has a reaction rate of $k^\circ = 1 \times 10^{-10}$ cm/s, the reaction rate for the ORR is $k^\circ \sim 1 \times 10^{-9}$ cm/s. Thus, the ORR is the kinetic rate-limiting half-reaction and its reaction rate must be increased for PEMFCs to be a viable alternative to combustion engines. Because cyclic voltammetry can be used to examine the kinetics of the ORR reaction, it is a critical technique in evaluating potential solutions to this problem.

Table 2.7.2 Summary of advantages and disadvantages of PEMFCs as an alternative to combustion engines.

| Advantages | Disadvantages |
|--|---|
| More efficient than combustion | ORR half-reaction too slow for commercial use |
| Greater energy density than fossil fuels | Hydrogen fuel is not readily available |
| Long-lasting | Water circulation must be managed to keep the proton exchange membrane hydrated |
| Reliable | |
| Quiet | |
| No harmful emissions | |

Cyclic Voltammetry

Overview

Cyclic voltammetry is a key electrochemical technique that, among its other uses, can be employed to examine the kinetics of oxidation-reduction reactions in electrochemical systems. Specifically, data collected with cyclic voltammetry can be used to determine the rate of reaction. In its simplest form, this technique requires a simple three electrode cell and a potentiostat Figure 2.7.14

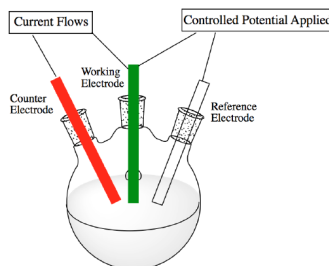


Figure 2.7.14 A simple three electrode cell.

A potential applied to the working electrode is varied linearly with time and the response in the current is measured Figure 2.7.14. Typically the potential is cycled between two values once in the forward direction and once in the reverse direction. For example, in Figure 2.7.15, the potential is cycled between 0.8V and -0.2V with the forward scan moving from positive to negative potential and the reverse scan moving from negative to positive potential. Various parameters can be adjusted including the scan rate, the number of scan cycles, and the direction of the potential scan i.e. whether the forward scan moves from positive to negative voltages or vice versa. For publication, data is typically collected at a scan rate of 20 mV/s with at least 3 scan cycles.

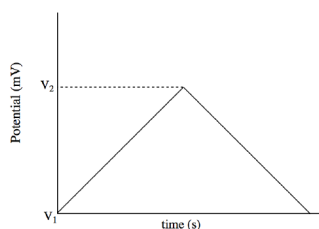


Figure 2.7.15 Triangular waveform demonstrating the cycling of potential with time.

Reading a Voltammogram

From a cyclic voltammetry experiment, a graph called a voltammogram will be obtained. Because both the oxidation and reduction half-reactions occur at the working electrode surface, steep changes in the current will be observed when either of these half-reactions occur. A typical voltammogram will feature two peaks where one peak corresponds to the oxidation half-reaction and the other to the reduction half-reaction. In an oxidation half-reaction in an electrochemical cell, electrons flow from the species in solution to the electrode resulting in an anodic current, i_a . Frequently, this oxidation peak appears when scanning from negative to positive potentials (Figure 2.7.16). In a reduction half-reaction in an electrochemical cell, electrons flow from the electrode to the species in solution, resulting in a cathodic current, i_c . This type of current is most often observed when scanning from positive to negative potentials. When the starting reactant is completely oxidized or completely reduced, peak anodic current, i_{pa} , and peak cathodic current, i_{pc} , respectively, are reached. Then, the current decays as the oxidized or reduced species leaves the electrode surface. The shape of these anodic and cathodic peaks can be modeled with the Nernst equation, 2.7.2, where number of electrons transferred and $E^{\circ'}$ (formal reduction potential) = $(E_{pa} + E_{pc})/2$

$$E_{eq} = E^{\circ'} + (0.059/n) \log ([reactant]/[product]) \quad (2.7.2)$$

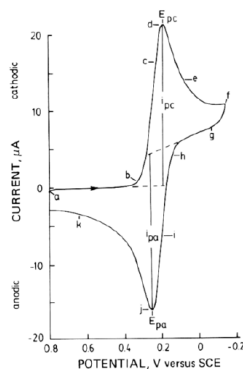


Figure 2.7.16 Example of an idealized cyclic voltammogram. Reprinted with permission from P. T. Kissinger and W. R. Heineman, *J. Chem. Educ.*, 1981, **60**, 702. Copyright 1983 American Chemical Society

Important Values from the Voltammogram

Several key pieces of information can be obtained through examination of the voltammogram including i_{pa} , i_{pc} , and the anodic and cathodic peak potentials. i_{pa} and i_{pc} both serve as important measures of catalytic activity: the larger the peak currents, the greater the activity of the catalyst. Values for i_{pa} and i_{pc} can be obtained through one of two methods: physical examination of the graph or the Randles-Sevcik equation. To determine the peak potentials directly from the graph, a vertical tangent line from the peak current is intersected with an extrapolated baseline. In contrast, the Randles-Sevcik equation uses information about the electrode and the experimental parameters to calculate the peak current, 2.7.3, where A = electrode area; D = diffusion coefficient; C = concentration; v = scan rate.

$$i_p = (2.69 \times 10^5) n^{3/2} A D^{1/2} C v^{1/2} \quad (2.7.3)$$

Anodic peak potential, E_{pa} , and cathodic peak potential, E_{pc} , can also be obtained from the voltammogram by determining the potential at which i_{pa} and i_{pc} respectively occur. These values are an indicator of the relative magnitude of the reaction rate. If the exchange of electrons between the oxidizing and reducing agents is fast, they form an electrochemically reversible couple. These redox couples fulfill the relationship: $\Delta E_p = E_{pa} - E_{pc} \approx 0.059/n$. In contrast, a nonreversible couple will have a slow exchange of electrons and $\Delta E_p > 0.059/n$. However, it is important to note that ΔE_p is dependent on scan rate.

Analysis of Reaction Kinetics

The Tafel and Butler-Volmer equations allow for the calculation of the reaction rate from the current-potential data generated by the voltammogram. In these analyses, the rate of the reaction can be expressed as two values: k° and i_0 . k° , the standard rate constant, is a measure of how fast the system reaches equilibrium: the larger the value of k° , the faster the reaction. The exchange current density, (i_0) is the current flow at the surface of the electrode at equilibrium: the larger the value of i_0 , the faster the reaction. While both i_0 and k° can be used, i_0 is more frequently used because it is directly related to the overpotential through the current-overpotential and Butler-Volmer equations. When the reaction is at equilibrium, k° and i_0 are related by 2.7.4, where $C_{o,eq}$ and $C_{R,eq}$ = equilibrium concentrations of the oxidized and reduced species respectively and a = symmetry factor.

$$i_O = nFk^\circ C_{O,eq}^{1-a} C_{R,eq}^a \quad (2.7.4)$$

Tafel equation

In its simplest form, the Tafel equation is expressed as 2.7.4, where a and b can be a variety of constants. Any equation which has the form of 2.7.5 is considered a Tafel equation.

$$E - E^\circ = a + b \log(i) \quad (2.7.5)$$

For example, the relationship between current, potential, the concentration of reactants and products, and k° can be expressed as 2.7.6, where $C_O(0,t)$ and $C_R(0,t)$ = concentrations of the oxidized and reduced species respectively at a specific reaction time, F = Faraday constant, R = gas constant, and T = temperature.

$$C_O(0,t) - C_R(0,t)e^{[nf/RT](E-E^\circ)} = [i/nFk^\circ][e^{[anF/RT](E-E^\circ)}] \quad (2.7.6)$$

At very large overpotentials, this equation reduces to a Tafel equation, 2.7.7, where $a = -[RT/(1-a)nF]\ln(i_0)$ and $b = [RT/(1-a)nF]$.

$$E - E^\circ = [RT/(1-a)nF]\ln(i) - [RT/(1-a)nF]\ln(i_0) \quad (2.7.7)$$

The linear relationship between $E - E^\circ$ and $\log(i)$ can be exploited to determine i_0 through the formation of a Tafel plot (Figure 2.7.17), $E - E^\circ$ versus $\log(i)$. The resulting anodic and cathodic branches of the graph have slopes of $[(1-a)nF/2.3RT]$ and $[-anF/2.3RT]$, respectively. An extrapolation of these two branches results in a y-intercept = $\log(i_0)$. Thus, this plot directly relates potential and current data collected by cyclic voltammetry to i_0 .

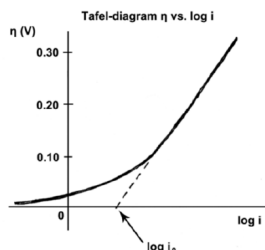


Figure 2.7.17 Example of an idealized Tafel plot. Reprinted with the permission of Dr. Rob C.M. Jakobs under the GNU Free Documentation License, Copyright 2010.

Butler-Volmer Equation

While the Butler-Volmer equation resembles the Tafel equation, and in some cases can even be reduced to the Tafel formulation, it uniquely provides a direct relationship between i_0 and H . Without simplification, the Butler-Volmer equation is known as the current-overpotential 2.7.8.

$$i/i_O = C_O(0,t)/C_{O,eq} e^{[anF/RT](E-E^\circ)} - [C_R(0,t)/C_{R,eq}] e^{[(1-a)nF/RT](E-E^\circ)} \quad (2.7.8)$$

If the solution is well-stirred, the bulk and surface concentrations can be assumed to be equal and 2.7.8 can be reduced to Butler-Volmer equation, 2.7.9.

$$I = i_O [e^{\{[anF/RT](E-E^\circ)\}} - e^{\{[(1-a)nF/RT](E-E^\circ)\}}] \quad (2.7.9)$$

Cyclic Voltammetry in ORR Catalysis Research

Platinum Catalysis

While the issue of a slow ORR reaction rate has been addressed in many ways, it is most often overcome with the use of catalysts. Traditionally, platinum catalysts have demonstrated the best performance at 30 °C, the ORR i_0 on a Pt catalyst is 2.8×10^{-7} A/cm² compared to the limiting case of ORR where $i_0 = 1 \times 10^{-10}$ A/cm². Pt is particularly effective as a catalyst for the ORR in PEMFCs because its binding energy for both O and OH is the closest to ideal of all the bulk metals, its activity is the highest of all the bulk metals, its selectivity for O₂ adsorption is close to 100%, and its extreme stability under a variety of acidic and basic conditions as well as high operating voltages Figure 2.7.18

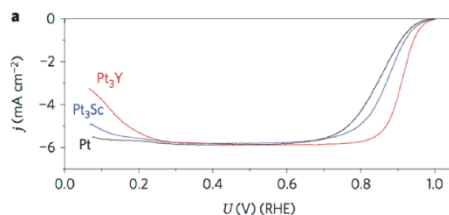


Figure 2.7.18 Anodic sweeps of cyclic voltammograms of Pt, Pt₃Sc, and Pt₃Y in 0.1 M HClO₄ at 20 mV/s. Reprinted by permission from Macmillan Publishers Ltd: [Nature] J. Greeley, I. E. L. Stephens, A. S. Bondarenko, T. P. Johansson, H. A. Hansen, T. F. Jaramillo, J. Rossmeisl, I. Chorkendorff, and J. K. Nørskov, *Nat. Chem.*, 2009, 1, 552. Copyright 2009.

Metal-Nitrogen-Carbon Composite Catalysis

Nonprecious metal catalysts (NPMCs) show great potential to reduce the cost of the catalyst without sacrificing catalytic activity. The best NPMCs currently in development have comparable or even better ORR activity and stability than platinum-based catalysts in alkaline electrolytes; in acidic electrolytes, however, NPMCs perform significantly worse than platinum-based catalysts.

In particular, transition metal-nitrogen-carbon composite catalysts (M-N-C) are the most promising type of NPMC. The highest-performing members of this group catalyze the ORR at potentials within 60 mV of the highest-performing platinum catalysts (Figure 2.7.19). Additionally, these catalysts have excellent stability: after 700 hours at 0.4 V, they do not show any performance degradation. In a comparison of high-performing PANI-Co-C and PANI-Fe-C (PANI = polyaniline), Zelenay and coworkers used cyclic voltammetry to compare the activity and performance of these two catalysts in H₂SO₄. The Co-PANI-C catalyst was found to have no reduction-oxidation features on its voltammogram whereas Fe-PANI-C was found to have two redox peaks at ~0.64 (Figure 2.7.20). These Fe-PANI-C peaks have a full width at half maximum of ~100 mV, which is indicative of the reversible one-electron Fe³⁺/Fe²⁺ reduction-oxidation (theoretical FWHM = 96 mV). Zelenay and coworkers also determined the exchange current density using the Tafel analysis and found that Fe-PANI-C has a significantly greater i_0 ($i_0 = 4 \times 10^{-8}$ A/cm²) compared to Co-PANI-C ($i_0 = 5 \times 10^{-10}$ A/cm²). These differences not only demonstrate the higher ORR activity of Fe-PANI-C when compared to Co-PANI-C, but also suggest that the ORR-active sites and reaction mechanisms are different for these two catalysts. While the structure of Fe-PANI-C has been examined (Figure 2.7.21) the structure of Co-PANI-C is still being investigated.

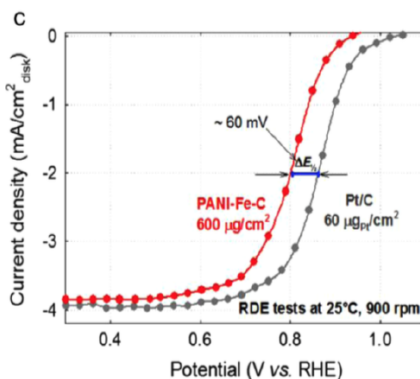


Figure 2.7.19 Comparison of Fe-PANI-C and Pt/C catalysts in basic electrolyte. Reprinted by permission from Macmillan Publishers Ltd: [Nature] H. T. Chung, J. H. Won, and P. Zelenay, *Nat. Commun.*, 2013, 4, 1922, Copyright 2013.

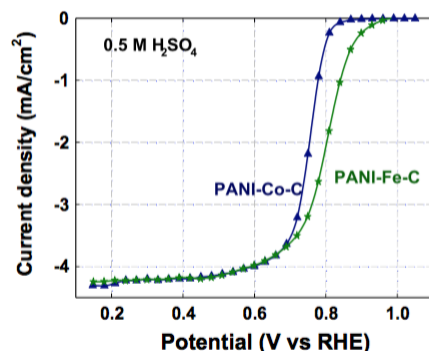


Figure 2.7.20 Comparison of Co-PANI-C and Fe-PANI-C catalysts by cyclic voltammetry for PANI-Fe-C catalysts. Reproduced from G. Wu, C.M. Johnston, N.H. Mack, K. Artyushkova, M. Ferrandon, M. Nelson, J.S. Lezama-Pacheco, S.D. Conradson, K.L. More, D.J. Myers, and P. Zelenay, *J. Mater. Chem.*, 2011, **21**, 11392-11405 with the permission of The Royal Society of Chemistry.

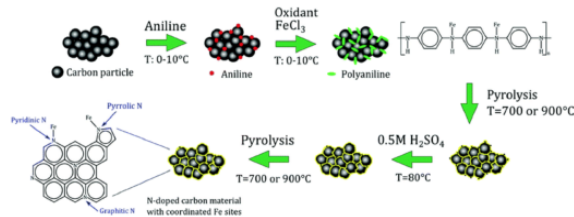


Figure 2.7.21 Synthetic scheme for Fe-PANI-C catalyst. Reprinted with the permission of the Royal Society of Chemistry under the CC BY-NC 3.0 License: N. Daems, X. Sheng, Y. Alvarez-Gallego, I. F. J. Vankelecom, and P. P. Pescarmona, *Green Chem.*, 2016, **18**, 1547. Copyright 2015.

While the majority of the M-N-C catalysts show some ORR activity, the magnitude of this activity is highly dependent upon a variety of factors; cyclic voltammetry is critical in the examination of the relationships between each factor and catalytic activity. For example, the activity of M-N-Cs is highly dependent upon the synthetic procedure. In their in-depth examination of Fe-PANI-C catalysts, Zelenay and coworkers optimized the synthetic procedure for this catalyst by examining three synthetic steps: the first heating treatment, the acid-leaching step, and the second heating treatment. Their synthetic procedure involved the formation of a PANI-Fe-carbon black suspension that was vacuum-dried onto a carbon support. Then, the intact catalyst underwent a one-hour heating treatment followed by acid leaching and a three-hour heating treatment. The heating treatments were performed at 900°C, which was previously determined to be the optimal temperature to achieve maximum ORR activity (Figure 2.7.21).

To determine the effects of the synthetic steps on the intact catalyst, the Fe-PANI-C catalysts were analyzed by cyclic voltammetry after the first heat treatment (HT1), after the acid-leaching (AL), and after the second heat treatment (HT2). Compared to HT1, both the AL and HT2 steps showed increases in the catalytic activity. Additionally, HT2 was found to increase the catalytic activity even more than AL (Figure 2.7.22). Based on this data, Zelenay and coworkers concluded HT1 likely either creates active sites in the catalytic surface while both the AL step removes impurities, which block the surface pores, to expose more active sites. However, this step is also known to oxidize some of the catalytic area. Thus, the additional increase in activity after HT2 is likely a result of “repairing” the catalytic surface oxidation.

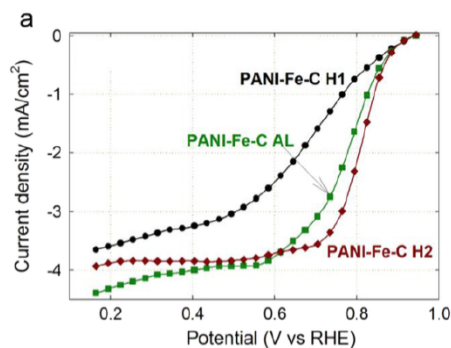


Figure 2.7.22 Comparison of synthetic techniques by cyclic voltammetry for PANI-Fe-C catalysts. Reproduced from G. Wu, C. M. Johnston, N. H. Mack, K. Artyushkova, M. Ferrandon, M. Nelson, J. S. Lezama-Pacheco, S. D. Conradson, K. L. More, D. J. Myers, and P. Zelenay, *J. Mater. Chem.*, 2011, **21**, 11392, with the permission of The Royal Society of Chemistry.

Conclusion

With further advancements in catalytic research, PEMFCs will become a viable and advantageous technology for the replacement of combustion engines. The analysis of catalytic activity and reaction rate that cyclic voltammetry provides is critical in comparing novel catalysts to the current highest-performing catalyst: Pt.

Chronocoulometry: A Technique for Electroplating

Fundamentals of Electrochemistry

A chemical reaction that involves a change in the charge of a chemical species is called an electrochemical reaction. As the name suggests, these reactions involve electron transfer between chemicals. Many of these reactions occur spontaneously when the various chemicals come in contact with one another. In order to force a nonspontaneous electrochemical reaction to occur, a driving force needs to be provided. This is because every chemical species has a relative reduction potential. These values provide information on the ability of the chemical to take extra electrons. Conversely, we can think of relative oxidation potentials, which indicate the ability of a chemical to give away electrons. It is important to note that these values are relative and need to be defined against a reference reaction. A list of standard reduction potentials (standard indicating measurement against the normal hydrogen electrode as seen in (Figure 2.7.23) for common electrochemical half-reactions is given in Table 2.7.3. Nonspontaneous electrochemical systems, often called electrolytic cells, as mentioned previously, require a driving force to occur. This driving force is an applied voltage, which forces reduction of the chemical that is less likely to gain an electron.

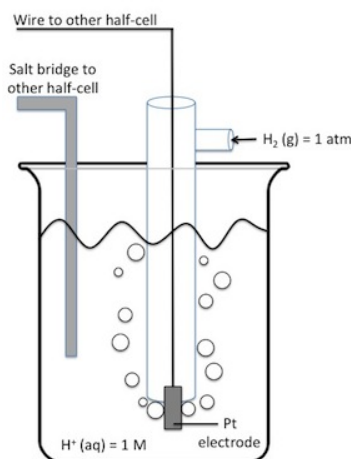


Figure 2.7.23 A schematic diagram of a normal hydrogen electrode.

Table 2.7.3 List of standard reduction potentials of various half reactions.

| Oxidant | Reductant | E° (V vs NHE) |
|--|---------------------------------------|---------------|
| $2\text{H}_2\text{O} + 2\text{e}^-$ | $\text{H}_2(\text{g}) + 2\text{OH}^-$ | -0.8227 |
| $\text{Cu}_2\text{O}(\text{s}) + \text{H}_2\text{O} + 2\text{e}^-$ | $2\text{Cu}(\text{s}) + 2\text{OH}^-$ | -0.360 |
| $\text{Sn}^{4+} + 2\text{e}^-$ | Sn^{2+} | +0.15 |
| $\text{Cu}^{2+} + 2\text{e}^-$ | $\text{Cu}(\text{s})$ | +0.337 |
| $\text{O}_2(\text{g}) + 2\text{H}^+ + 2\text{e}^-$ | $\text{H}_2\text{O}_2(\text{aq})$ | +0.70 |

Design of an Electrochemical Cell

A schematic of an electrochemical cell is seen in Figure 2.7.24. Any electrochemical cell must have two electrodes – a cathode, where the reduction half-reaction takes place, and an anode, where the oxidation half-reaction occurs. Examples of half reactions can be seen in Table 2.7.3. The two electrodes are electrically connected in two ways – the electrolyte solution and the external wire. The electrolyte solution typically includes a small amount of the electroactive analyte (the chemical species that will actually participate in electron transfer) and a large amount of supporting electrolyte (the chemical species that assist in the movement of charge, but are not actually involved in electron transfer). The external wire provides a path for the electrons to travel from the oxidation half-reaction to the reduction half-reaction. As mentioned previously, when an electrolytic reaction (nonspontaneous) is

being forced to occur a voltage needs to be applied. This requires the wires to be connected to a potentiostat. As its name suggests, a potentiostat controls voltage (i.e., “potentio” = potential measured in volts). The components of an electrochemical cell and their functions are also given in Table 2.7.4.

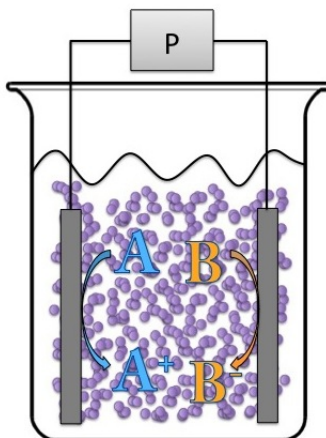


Figure 2.7.24 Schematic of an electrochemical cell.

Table 2.7.4 Various components of an electrochemical cell and their respective functions.

| Component | Function |
|------------------------|--|
| Electrode | Interface between ions and electrons |
| Anode | Electrode at which the oxidation half reaction takes place |
| Cathode | Electrode at which the reduction half reaction takes place |
| Electrolyte solution | Solution that contains supporting electrolyte and electroactive analyte |
| Supporting electrolyte | Not a part of the faradaic process; only a part of the capacitive process |
| Electroactive analyte | The chemical species responsible for all faradaic current |
| Potentiostat | DC Voltage source; sets the potential difference between the cathode and anode |
| Wire | Connects the electrodes to the potentiostat |

Chronocoulometry: an Electroanalytical Technique

Theory

Chronocoulometry, as indicated by the name, is a technique in which the charge is measured (i.e. “coulometry”) as a function of time (i.e., “chrono”). There are various types of coulometry. The one discussed here is potentiostatic coulometry in which the potential (or voltage) is set and, as a result, charge flows through the cell. The input and output example graphs can be seen in Figure 2.7.25. The input is a potential step that spans the reduction potential of the electroactive species. If this potential step is performed in an electrochemical cell that does not contain an electroactive species, only capacitive current will flow (Figure 2.7.26), in which the ions migrate in such a way that charges are aligned (positive next to negative, but no charge is transferred). Once an electroactive species is introduced into the system however, the faradaic current begins to flow. This current is a result of the electron transfer between the electrode and the electroactive species.

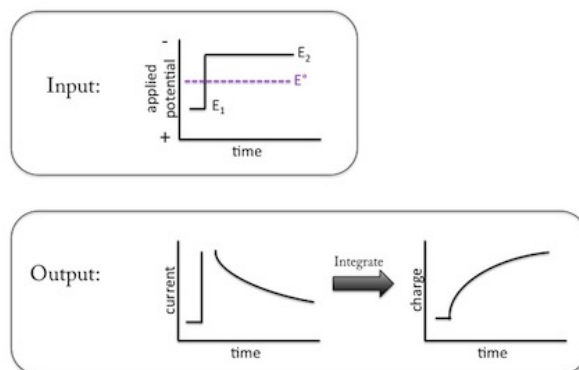


Figure 2.7.25 Input potential step (a) and output charge transfer (b) as used in chronocoulometry.

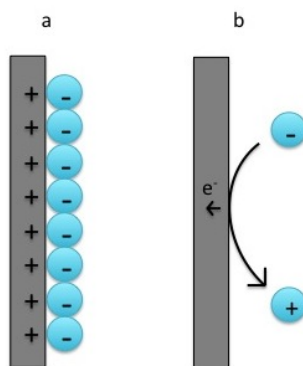


Figure 2.7.26 Capacitive alignment (a) and faradaic charge transfer (b) – the two sources of current in an electrochemical cell.

Electroplating: an Application of Chronocoulometry

Electroplating is an electrochemical process that utilizes techniques such as chronocoulometry to electrodeposit a charged chemical from a solution as a neutral chemical on the surface of another chemical. These chemicals are typically metals. The science of electroplating dates back to the early 1800s when Luigi Valentino Brugnatelli (Figure 2.7.27) electroplated gold from solution onto silver metals. By the mid 1800s, the process of electroplating was patented by cousins George and Henry Elkington (Figure 2.7.28). The Elkingtons brought electroplated goods to the masses by producing consumer products such as artificial jewelry and other commemorative items (Figure 2.7.29).



Figure 2.7.27 Portrait of Luigi Valentino Brugnatelli (1761-1818).



Figure 2.7.28 Portrait of George Elkington (1801-1865)



Figure 2.7.29 A commemorative inkstand gilded using the process of electroplating.

Recent scientific studies have taken interest in studying electroplating. Trejo and coworkers have demonstrated that a quartz microbalance can be used to measure the change in mass over time during electrodeposition via chronocoulometry. Figure 2.7.30a shows the charge transferred at various potential steps. Figure 2.7.30b shows the change in mass as a function of potential step. It is clear that the magnitude of the potential step is directly related to the amount of charge transferred and consequently the mass of the electroactive species deposited.

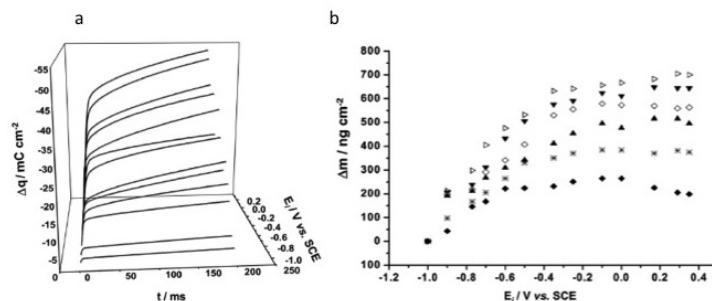


Figure 2.7.30 Charge transferred over time at varied potentials (a) and mass transferred at varied potentials. Reproduced from A. Mendez, L. E. Moron, L. Ortiz-Frade, Y. Meas, R. Ortega-Borges, G. Trejo, *J. Electrochem. Soc.*, 2011, **158**, F45. Copyright: The Electrochemical Society, 2011.

The effect of electroplating via chronocoulometry on the localized surface plasmon resonance (LSPR) has been studied on metallic nanoparticles. An LSPR is the collective oscillation of electrons as induced by an electric field (Figure 2.7.31). In various studies by Mulvaney and coworkers, a clear effect on the LSPR frequency was seen as potentials were applied (Figure 2.7.32). In initial studies, no evidence of electroplating was reported. In more recent studies by the same group, it was shown that nanoparticles could be electroplated using chronocoulometry (Figure 2.7.33). Such developments can lead to an expansion of the applications of both electroplating and plasmonics.

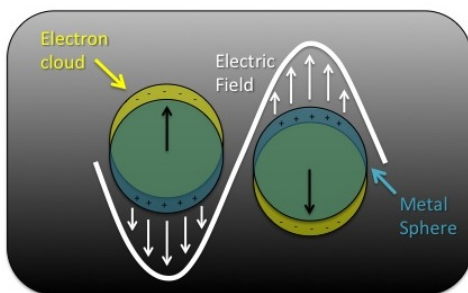


Figure 2.7.31 The localized surface plasmon resonance as induced by application of an electric field.

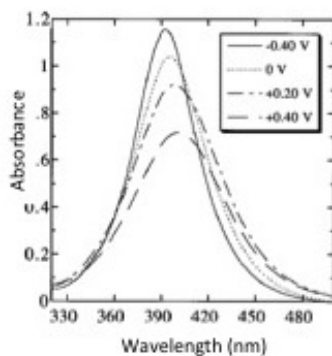


Figure 2.7.32 Shift in the localized surface plasmon resonance frequency as a result of applied potential step. Reproduced from T. Ung, M. Giersig, D. Dunstan, and P. Mulvaney, *Langmuir*, 1997, **13**, 1773. Copyright: American Chemical Society, 1997.

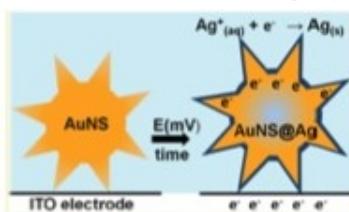


Figure 2.7.33 Use of chronocoulometry to electroplate nanoparticles. Reproduced from M. Chirea, S. Collins, X. Wei, and P. Mulvaney, *J. Phys. Chem. Lett.*, 2014, **5**, 4331. Copyright: American Chemical Society, 2014

This page titled [2.7: Electrochemistry](#) is shared under a [CC BY 4.0](#) license and was authored, remixed, and/or curated by [Pavan M. V. Raja & Andrew R. Barron \(OpenStax CNX\)](#) via [source content](#) that was edited to the style and standards of the LibreTexts platform.